A Structural Health Monitoring Approach based on Contact Acoustic Nonlinearity and Its Application to Quantitative Evaluation of Fatigue Cracks

Kai WANG[1] and Zhongqing SU[*1,2]

[1] Department of Mechanical Engineering, The Hong Kong Polytechnic University, Hong Kong SAR
[2] The Hong Kong Polytechnic University Shenzhen Research Institute, Shenzhen 518057, P.R. China

[*] zhongqing.su@polyu.edu.hk

Key words: contact acoustic nonlinearity (CAN); fatigue crack; second harmonic generation; structural health monitoring.

Abstract

A damage characterization approach was developed in this study by exploiting the second harmonics generated owing to the interaction between incident Lamb waves and a *"breathing" crack. The* approach can be expanded to deployment of structural health monitoring, whereby fatigue cracks in a plate-like structure can be evaluated quantitatively. A dedicated analytical model, in conjunction with the use of a variational principle-based method and an elasto-dynamic reciprocity method, was established. Using the model, an insight into the modulation mechanism of the crack on Lamb wave propagation was achieved, and the contact acoustic nonlinearity (CAN)-induced second harmonic generation was interrog*ated. Two scenarios were considered in which the plate bearing a "breathing" crack* was modelled in two-dimensional and three-dimensional scenarios, respectively, yielding a quantitative correlation between crack parameters and second harmonic-based nonlinearity index. Results obtained from the proposed approach were compared with those from finite element simulation, to observe good coincidence.

1 INTRODUCTION

Amongst currently prevailing structural health monitoring (SHM) methods, e.g. eddy-current, infrared thermography, and X-ray-based methods, guided waves-based SHM [1, 2] is deemed one of the most promising candidates owing to its advantageous characteristics including long range inspection, high sensitivity and low energy consuming. Lamb waves are a representative type of guided waves, existing in a plate or a shell-like structure. Traditionally, most Lamb-waves-based SHM methods [3-5] have been developed based on discerning and analysing linear changes in wave features (e.g. reflection/transmission, time-of-flight, mode conversions), whereby the location and severity of damage can be estimated qualitatively or quantitatively. However experimental observations and analytical studies have increasingly argued that the sensitivity of those linear wave feature-based methods are limited, especially when used to detect damage whose sizes are smaller than the wavelength of the incident waves. This limitation has entailed intensive exploration on the use of nonlinear wave features based-methods [6-9], which exploit the shift of energy from the

incident frequency to other frequency bands, e.g. generation of higher order harmonics.

A rich body of literatures has illustrated the source of nonlinearity in the propagating waves, such as material nonlinearity [10] and contact acoustic nonlinearity (CAN) [11]. With regard to the material nonlinearity, the requirement for continuous accumulation of nonlinearity in the waves, i.e. the phase velocities of the fundamental waves and second harmonic being equivalent with non-zero power flow, impinges limitation on the choice of the incident waves. Besides, the characteristic that the detected nonlinearity, as an accumulated feature, is caused by the medium between the actuator and sensor implies that the material nonlinearity can only indicates the presence of damage in the medium and fails to locate the site of the damage. During long-term service, especially when subjected to cyclically repeating load, fatigue cracks can be developed in engineering structures whereby the effect of CAN from fatigue cracks inclines to dominate the nonlinearity in the propagating waves.

With the recognition that the CAN is generated owing to the presence of the "breathing" crack, Soldove et al. [11] applied a CAN model to interpret the influence of a "breathing" crack on the propagation of waves and consequently the generation of higher-order harmonics. In this method the crack was defined with a specific material in which a stepwise change in material stiffness was assumed. Richardson [12] investigated a similar problem by scrutinizing the behaviour of the interface. These studies, conducted in one-dimensional scenario, have their merits in providing analytical interpretation for the generation of higher-order harmonics in a quantitative manner. However, when extended to two-dimensional (2D) or three-dimensional (3D) scenarios, these methods may show the limitation. In 2D and 3D scenarios, reflection/transmission of the incident waves induced by the "breathing" crack are accompanied not only by the evanescent modes, but also by the converted modes and diffracted modes radiated from the crack tips [13]. Another paramount challenge for achieving an analytical insight into the interpretation of the modulation mechanism of a "breathing" crack on the propagation of Lamb waves in the 2D and 3D problems originates from the difficulty in solving the governing equation due to the time-varying boundary conditions.

Motivated by this, an analytical model dedicated to interpreting the modulation mechanism of a "breathing" crack on the propagation of waves and the generation of higher-order harmonics in 2D and 3D scenarios was developed. In this model, the crack when waves are traversing is modelled as a second source for the wave excitation in the medium, and the crack-induced second source stress (CISS) was investigated and analysed in terms of both time duration and space distribution. With the CISS, amplitude of the crack-induced second harmonics can be obtained by applying a variant principle-based method and an elasto-dynamic method in the 2D and 3D cases, respectively, whereby a proposed nonlinearity index related with parameters of the "breathing" crack was constructed to quantitatively represent the severity of the crack. Results obtained from the proposed model were compared with those from the finite element method (FEM) simulation, to observe good coincidence.

2 MODULATION MECHANISM OF "BREATHING" CRACK ON WAVES IN 2D SCENARIO

Considering a two-dimensional infinite plate bearing a "breathing" crack, when the crack closes, compressive and shear stress of Lamb waves are transmitted and no CISS is generated; when the crack opens during dilation when the waves are traversing., as shown in Fig. 1, the CISS is induced and thereby waves are partially decoupled. It is the CISS induced by

interaction of the open crack with Lamb waves that generates the reflection and transmission; and it is such a time-dependent feature of the CISS caused by the "breathing" behaviour of the crack leads to the generation of CAN manifested in the propagating waves, as typified by the second harmonic.

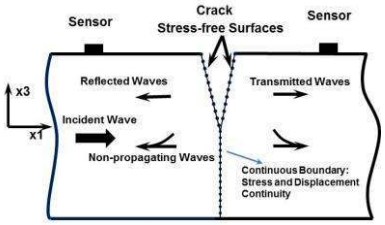

Figure 1: Schematic of a two-dimensional infinite plate bearing a "breathing" crack when the crack is open

During crack opening, the influence of the open crack on the propagation of the waves is identical to that of a notch with the same geometrical parameters. A modal decomposition method [14] was employed to obtain the amplitude of each mode generated by the interaction of the Lamb waves with the open crack. The stress and displacement fields of these modes form a complete basis that stress and displacement field with any distribution can be expressed as the superposition of these modes. Thus, the boundary conditions on the crack surfaces during the crack opening can be expressed as follows

$$\begin{matrix}\sigma_{11}\\ \sigma_{13}\end{matrix} = \begin{cases}\sum_N b_N \sigma_{11}^N\\ \sum_N b_N \sigma_{13}^N\end{cases} = \begin{cases}0\\ 0,\end{cases} \text{ stress free at the right surface of crack} \tag{1}$$

$$\begin{matrix}\sigma_{11}\\ \sigma_{13}\end{matrix} = \begin{cases}b_{Inc}\sigma_{11}^{Inc} + \sum_N b_{-N}\sigma_{11}^{-N}\\ b_{Inc}\sigma_{13}^{Inc} + \sum_N b_{-N}\sigma_{13}^{-N}\end{cases} = \begin{cases}0\\ 0,\end{cases} \text{ stress free at the left surface of crack} \tag{2}$$

$$\sum_N b_N u^N = b_{Inc} u^{Inc} + \sum_N b_{-N} u^{-N}, \text{ displacement continuity at continuous boundary} \tag{3}$$

$$\begin{matrix}\sum_N b_N \sigma_{11}^N\\ \sum_N b_N \sigma_{33}^N\\ \sum_N b_N \sigma_{13}^N\end{matrix} = \begin{cases}b_{Inc}\sigma_{11}^{Inc} + \sum_N b_{-N}\sigma_{11}^{-N}\\ b_{Inc}\sigma_{33}^{Inc} + \sum_N b_{-N}\sigma_{33}^{-N}\\ b_{Inc}\sigma_{13}^{Inc} + \sum_N b_{-N}\sigma_{13}^{-N}.\end{cases} \text{ stress continuity at continuous boundary} \tag{4}$$

In the above, N is an index of propagating and non-propagating modes, and $-N$ indicates the modes propagating opposite to the incident wave. σ^N and u^N denote the stress and displacement fields induced by the N^{th} wave mode, respectively. Coefficient b_N is the unknown complex magnitude to be correlated with the magnitude of the incident wave which is denoted by b_{Inc}. σ^{Inc} and u^{Inc} are the stress and displacement fields induced by the incident waves, respectively.

Upon solving Eqs. (1)–(4) using a singular value decomposition method, the magnitude of each mode can be obtained and therefore the displacement and stress fields at the crack can be depicted as follows:

$$u_1^-(x_3,t) = b_{Inc}u^{Inc} + \sum_N b_{-N}u^{-N},\ u_1^+(x_3,t) = \sum_N b_N u^N, \tag{5}$$

$$\sigma_{11}^{Crack-} = b_{Inc}\sigma_{11}^{Inc} + \sum_N b_{-N}\sigma_{11}^{-N},\quad \sigma_{11}^{Crack+} = \sum_N b_N \sigma_{11}^N,$$

where $\sigma^{\text{Crack}-}$ ($\sigma^{\text{Crack}+}$) is the stress field at the crack induced by the incident waves and the reflected waves (transmitted waves). u_1^+ and u_1^- denote the in-plane displacements of points on the right (transmitted) and left (reflected) stress-free surface of the crack, respectively. Given the stress field when the crack opens, the CISS which is defined as the deviation of the stress field induced by the open crack from that in a pristine plate can be yielded as follows:

$$\sigma^{\text{ref}} = \sigma^{\text{ref}}\left(x_3\right)e^{iwt} = \left(\sigma^{\text{Crack}-} - b_{\text{Inc}}\sigma^{\text{Inc}}\right)e^{iwt}. \tag{6}$$

In the above, σ^{ref} represents the crack-induced stress field in the reflection.

2.1 Frequency analysis

When the Lamb waves traversing a "breathing" crack, the crack closes and opens periodically. The crack opens at the moment when the phase of the stress field at the crack interface turns from compression into tension. This moment is denoted as t_{open}, and the duration between two consecutive crack opening is the period of the Lamb waves. Upon the crack opening, the displacement of the crack surfaces can be expressed by Eq. (5). Setting the gap between the two crack surfaces as zero gives the moment, denoted by t_{close} when the crack closes and the reflection/transmission ceases. The gap can be depicted as:

$$\Delta = u_1^+\left(x_3, t_{\text{close}}\right) - u_1^-\left(x_3, t_{\text{close}}\right) = 0. \tag{7}$$

As said earlier, the reflection/transmission of the incident Lamb wave is present during crack opening or absent otherwise. This phenomenon can be treated as a scenario in which the crack-induced stress field in an open crack case is modulated by a periodic window function, as

$$f\left(t\right) = \begin{cases} 1, & t_{\text{open}} < t < t_{\text{close}} \\ 0, & t_{\text{close}} < t < t_{\text{open}} + T_{\text{inc}}, \end{cases} \tag{8}$$

where T_{inc} is the period of the incident wave. Therefore, the stress field induced by the "breathing" crack in the reflection, can be obtained as

$$\sigma_{11}^{\text{ref}} = \sigma_{11}^{\text{ref}}\left(x_3\right)e^{iwt} \times f\left(t\right), \quad \sigma_{13}^{\text{ref}} = \sigma_{13}^{\text{ref}}\left(x_3\right)e^{iwt} \times f\left(t\right). \tag{9}$$

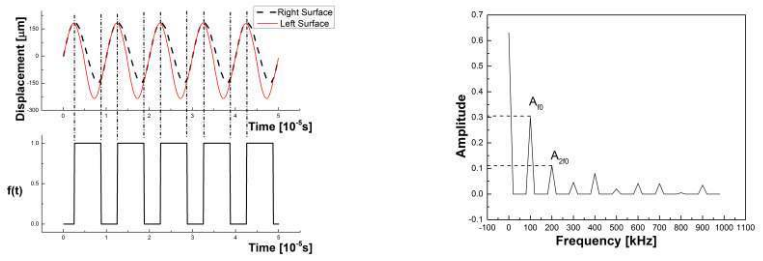

(a) (b)

Figure 2: (a) Modulating function based on Eq. (8); and (b) Spectrum of the crack-induced stress field

The corresponding spectrum of the crack-induced stress field can be obtained using the convolution between the incident wave period function e^{iwt} and a window function $f\left(t\right)$. In the spectrum, the magnitude of each component can be ascertained. To summarize, the above

process can be illuminated in Fig. 2.

2.2 Analysis of propagating modes generated at the double frequency

In order to achieve an insight into the consequently generated propagating harmonics at double frequency in the reflection/transmission wave fields, a method based on the variational principle [15] was employed. In this method, the crack-induced stress field, as expressed in Eq. (6), was deemed as an additional excitation source to induce wave reflection/transmission. Knowing the magnitude of the crack-induced stress source at double frequency, i.e. A_{2f_0}, the CISS can be yielded as

$$\sigma^{\text{ref}-2f_0} = A_{2f_0}\sigma^{\text{ref}}\left(x_3\right)e^{i2wt} = A_{2f_0}\left(\sigma^{\text{Crack}-} - b_{\text{Inc}}\sigma^{\text{Inc}}\right)e^{i2wt}. \tag{10}$$

In the above, $\sigma^{\text{ref}-2f_0}$ denotes the crack-induced stress source at double frequency at the crack surface.

In this study, the 2D infinite plate bearing a crack was deemed as two semi-infinite parts tied together via the continuous boundary at the site of crack, and the CISS with the above distribution was applied at the boundaries of the two parts left and right to the crack, serving as an additional excitation source. Using the method based on variational principle, the generated wave modes can be obtained as follows:

$$[b_n] = [R_{nm}] \bullet \frac{1}{h}\int_{-h}^{h}\left(u_1^m\bar{T}_1 + u_3^m\bar{T}_3\right)dx_3, \tag{11}$$

$$[R] = \left[\frac{1}{h}\int_{-h}^{h}\left(u_1^m\bar{\sigma}_{11}^n + u_3^m\bar{\sigma}_{13}^n\right)dx_3\right]^{-1}.$$

In the above, $[b_n]$ is the vector of the magnitude of each wave mode generated by the crack-induced stress source, $\bar{T}_1 = \bar{\sigma}_{11}^{\text{ref}-2f_0}$ and $\bar{T}_3 = \bar{\sigma}_{13}^{\text{ref}-2f_0}$. u_1^m and u_3^m denote the in-plane and out-of-plane displacement fields of the m^{th} mode at the double frequency, respectively. $\bar{\sigma}^n$ is the conjugate of the stress field of the n^{th} mode. h is the half-thickness of the plate.

With the accordingly obtained magnitudes of the crack-generated propagating modes, a dimensionless damage index was proposed, to calibrate the severity of the fatigue crack by

$$\text{NI} = \frac{b_1^{2f_0}u_1^{2f_0}(h)}{b_{\text{Inc}}u_1^{f_0}(h)}, \tag{12}$$

where NI denotes the nonlinearity index, which is the ratio of magnitude of the displacement induced by the reflected propagating-mode at double frequency to the magnitude of that induced by the incident waves. $u_1^{f_0}(h)$ and $u_1^{2f_0}(h)$ are the mode shape functions for the in-plane displacements at the incident and double frequencies, respectively. $b_1^{2f_0}$ denotes the magnitude of the crack-induced propagating mode at double frequency.

3 MODULATION MECHANISM OF "BREATHING" CRACK ON WAVES IN 3D SCENARIO

Extending the above model to 3D scenario, a plate with a through-thickness crack was investigated. The "breathing" behaviour of the crack under the modulation of the incident waves is similar to that in the 2D scenario, however additional complexity is introduced. For

example, more wave modes, e.g. shear horizontal waves (SH), are induced, and diffraction radiated from the crack tips also influences the stress fields in the medium [11].

In the model, a point-like force is applied in the symmetric plane normal to the crack, and the site of the sensor is also in the plane, as shown in Fig. 3(a). Applying the similar analysis procedures stated in the 2D scenario, the modulation mechanism of a "breathing" crack on the Lamb waves can be interpreted, whereby the generation of higher-order harmonics can be predicted in a quantitative manner.

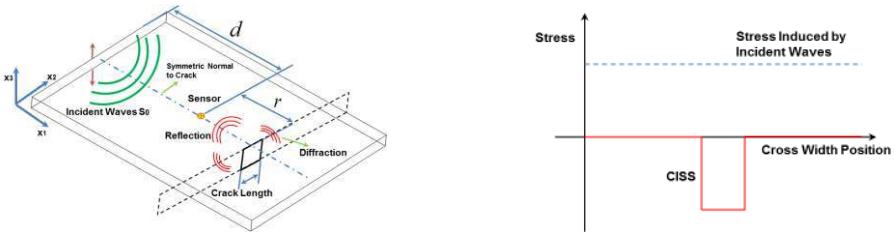

(a) (b)

Figure 3: (a) Details of the configuration studied; (b) CISS in the plane containing the crack

It has been found that the CISS generated in the crack surfaces is the anti-symmetric counterpart of the stress field induced by the probing Lamb waves. The CISS outside the crack surfaces in the plane containing the crack is, in principle, zero (except the limited zone near the tips, whose influence can be ignored), as shown in Fig. 3(b). Because the scale of the crack in this study, measuring half of the wavelength of the incident Lamb waves at its maximum, can be ignored compared with the distance between the sensors and the crack, the CISS can be regarded as a point force with the magnitude equivalent to the following integration of the CISS over the crack surface.

$$T = \int_{\text{Crack Surface}} -\sigma^{\text{inc}} ds. \tag{13}$$

The amplitude of the propagating wave mode to be captured by the sensor can be acquired, using an elasto-dynamic method [16], as a function of the coordinates of the inspecting sensors, as follows:

$$u_{x_i} = A_m^S V_S^m(x_3)\left[H_0^2(k_m r) - \frac{1}{k_m r} H_1^2(k_m r)\right], \tag{14}$$

$$A_m^S = \frac{k_m}{4i} \frac{T V_S^m(x_3^0)}{I_{mm}^S}.$$

In the above, A_m^S and k_m denote the amplitude and wavenumber of the m^{th} propagating symmetric mode of Lamb waves, respectively. r denotes the distance between the sensor and the crack. H_0^2 and H_1^2 represent the Hankle function of the zero order and first order, respectively. V_S^m and I_{mm}^S have the same definition as in reference [16].

In order to gain an insight into the generation of higher-order harmonics, an approximation about the duration of the crack opening was proposed. This approximation was based on the examination of the depending factors for the crack opening displacement (COD), i.e. the CISS in the crack surfaces and diffractions radiated from the crack tips. The duration of the crack opening induced by the CISS in the crack surfaces, is consistent with

half period of the CISS, i.e. half period of the incident waves $T_{inc}/2$; and the duration caused by diffraction radiated from the crack tips can be estimated with the propagation time from the crack tip to the symmetric plane of the crack, i.e. $LT_{inc}/2\lambda_{SH}$, leading to the consequence that total duration can be approximated as $LT_{inc}/2\lambda_{SH}+T_{inc}/2$, where L is the crack length and λ_{SH} denotes the wavelength of the diffracted SH waves. Similar to the 2D scenario, the modulation function $f(t)$ can be defined, as shown in Fig. 4, and the spectrum of the CISS can be evaluated as follows:

$$T=\int_{\text{Crack Surface}}-\sigma^{inc}ds\,e^{iwt}\times f(t), \tag{15}$$

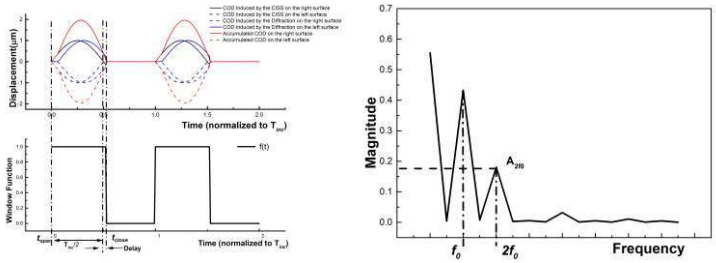

(a) (b)

Figure 4: (a) Approximated modulation function; (b) spectrum of the CISS

With the obtained spectrum and the amplitude of the CISS, the displacement field caused by the CISS at double frequency can be predicted by substituting the load in Eq. (15) with the following:

$$T_{2f_0}=A_{2f_0}\times\int_{\text{Crack Surface}}-\sigma^{inc}ds. \tag{16}$$

Similarly, an index, which is related to the parameters of the crack, can be defined to indicate the nonlinearity manifested in the propagating waves:.

$$NI^{3D}=\frac{u_{x_1}^{2f_0}}{u_{x_1}^{f_0}}, \tag{17}$$

where $u_{x_1}^{2f_0}$ is the CISS-induced displacement at double frequency and $u_{x_1}^{f_0}$ is the displacement induced by incident waves at incident frequency. It is worth noting that the waves in the model decay cylindrically away from the source so the signals were compensated accordingly for beam spreading such that the influence of the decay of the incident waves can be eliminated, yielding

$$NI_{\text{point load}}^{3D}=NI^{3D}\times\frac{\sqrt{d+r}}{\sqrt{d}} \tag{18}$$

In the above, d denotes the distance between the source of incident waves and the sensor.

4 VALIDATION USING FINITE ELEMENT METHOD

4.1 Validation of the proposed model in 2D scenario

For validation of the proposed model in 2D scenario, an aluminium plate, measuring 8 mm in thickness and 1000 mm in length, was meshed and analysed with ABAQUS®/EXPLICIT. The properties of the aluminium plate are listed in Table 1.

Density (kg/m^3)	E (GPa)	υ	c_L (m/s)	c_T (m/s)
2660	71.8	0.33	6324	3185

Table 1. Properties of Aluminum Plate

For the discussed crack in the plate thickness, the symmetric propagating mode (S0) was chosen as the incident wave to make use of its higher sensitivity to this type of crack than an antisymmetric mode, because its in-plane displacement dominates the signal energy. The incident five-cycle Hanning-windowed sinusoidal tone bursts were produced by applying the cross-thickness displacement field of pure S0 mode at incident frequency. To model the "breathing" crack in the plate, the stress-free surfaces of the crack were defined as a seam crack, and a contact-pair interaction between the two crack surfaces was applied.

Applied with the short-time Fourier Transform (STFT) analysis, the time-frequency spectra of the captured Lamb waves can be obtained. Fig. 5(a), (b) representatively show the spectra when crack depth is 50% and 75% of the plate thickness. From the spectra, each wave mode can be distinguished and their respective magnitudes can be extracted to calculate the index using Eq. (13).

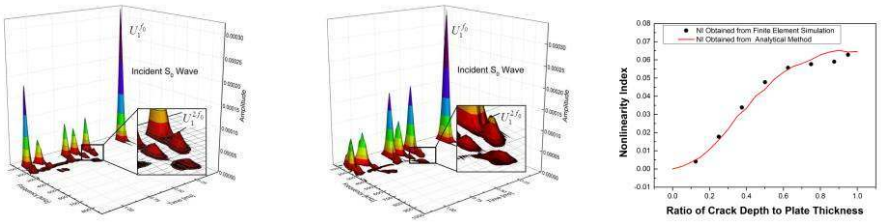

(a) (b) (c)

Figure 5: Spectra of the captured signals when ratio of crack depth to thickness is: (a) 50%; and (b) 75%; (c) nonlinearity index against ratio of crack depth to the plate thickness for the "breathing" crack

The accordingly obtained correlation between the defined index and crack parameters was established， as shown in Fig. 5(c), compared with the results obtained from the analytical method, to observe good coincidence.

4.2 Validation of the proposed model in 3D scenario

Analogously, a plate measuring 2mm in thickness, 500mm in length and 600mm in width was analysed with ABAQUS®/EXPLICIT. The properties of the aluminium plate are identical to those listed in Table 1. The incident waves and definition for the crack were identical to that in 2D scenario. In order to make the second harmonics caused by the "breathing" crack evident, the simulations for each crack length were conducted twice with the same settings, except for the point force applied to induce the incident waves in one case was the inverse of that applied in another case. By adding up the recorded signals in both

cases, the component with the incident frequency was eliminated while the component with double frequency was doubled, as shown in Fig. 6(a), (c).

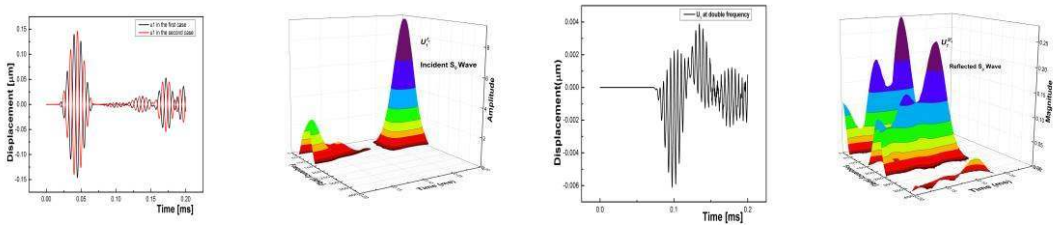

(a) (b) (c) (d)

Figure 6: (a) Recorded displacement along x_1 axis; (b) spectra of the captured signals; (c) superposition of the recorded signal in (a); (d) spectra of the superposed signal

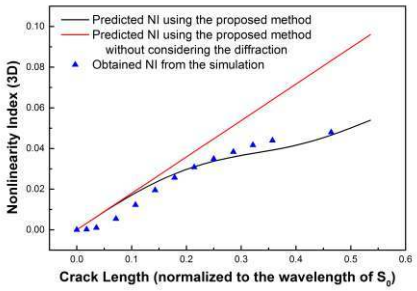

Figure 7: Nonlinearity index (in 3D scenario) against the crack length (normalized to the wavelength of S_0)

Using the same processing method as that in 2D scenario, the obtained correlation between the defined index and crack parameters was established, in Fig. 7, compared with the results obtained from the analytical method. It is demonstrated from Fig. 5(c) and Fig. 7 that the severer a crack is the larger the defined nonlinearity index it will be, and the diffraction has a significant influence of on the generated nonlinearity. From the monotonous correlation shown in Fig. 5(c) and Fig. 7, conclusion can be drawn that the NI can be used to represent the severity of the crack damage.

5 DISCUSSION AND CONCLUSION

This study proposed a dedicated analytical model to interpret the modulation mechanism of a "breathing" crack on the propagation of incident Lamb waves, and interrogate the generation of CAN-induced second harmonics. In this model, the crack was deemed as a second source for wave excitation, and the CISS induced by the "breathing" behaviour was scrutinised, whereby the spectra of the source for additional wave excitation can be obtained. In conjunction with a variant principle-based method and an elasto-dynamic method in 2D and 3D scenario respectively, the displacement field induced by the "breathing" crack at double frequency can be ascertained. With accordingly obtained results, a nonlinearity index linked with the crack parameters was proposed to represent the severity of the crack. Results obtained from the proposed approach were compared with those from FE simulations and good coincident were observed.

ACKNOWLEDGEMENT

This project is supported by the Hong Kong Research Grants Council via General

Research Funds (No. 523313 and No. 15214414). This project is also supported by National Natural Science Foundation of China (Grant No. 51375414).

REFERENCES

[1] M. Lowe, P. Cawley, J. Kao, and O. Diligent, Prediction and measurement of the reflection of the fundamental anti-symmetric Lamb wave from cracks and notches, REVIEW OF PROGRESS IN QUANTITATIVE NONDESTRUCTIVE EVALUATION, **19**,193-200 (2000).

[2] Z. Su and L. Ye, Identification of damage using Lamb waves: from fundamentals to applications, Springer Science & Business Media, 48(2009).

[3] A. Raghavan and C. E. Cesnik, Review of guided-wave structural health monitoring, Shock and Vibration Digest, **39**, 91-116 (2007).

[4] J. Pei and M. Deng, Assessment of fatigue damage in solid plates using ultrasonic lamb wave spectra, Ultrasonics Symposium, 2008. IUS 2008. IEEE,1869-1872 (2008).

[5] Y. Lu, L. Ye, Z. Su, and C. Yang, Quantitative assessment of through-thickness crack size based on Lamb wave scattering in aluminium plates, Ndt & E International, **41**, 59-68 (2008).

[6] C. Zhou, M. Hong, Z. Su, Q. Wang, and L. Cheng, Evaluation of fatigue cracks using nonlinearities of acousto-ultrasonic waves acquired by an active sensor network, Smart Materials and Structures, **22**, 015018 (2012).

[7] G. Zumpano and M. Meo, A new nonlinear elastic time reversal acoustic method for the identification and localisation of stress corrosion cracking in welded plate-like structures–A simulation study, International journal of solids and structures, **44**, 3666-3684 (2007).

[8] C. Pruell, J.-Y. Kim, J. Qu, and L. J. Jacobs, Evaluation of fatigue damage using nonlinear guided waves, Smart Materials and Structures, **18**, 035003 (2009).

[9] A. Klepka, W. Staszewski, R. Jenal, M. Szwedo, J. Iwaniec, and T. Uhl, Nonlinear acoustics for fatigue crack detection–experimental investigations of vibro-acoustic wave modulations, Structural Health Monitoring, **11**, 197-211 (2012).

[10] J. Kober and Z. Prevorovsky, Theoretical investigation of nonlinear ultrasonic wave modulation spectroscopy at crack interface, NDT & E International, **61**, 10-15 (2014).

[11] I. Y. Solodov, N. Krohn, and G. Busse, CAN: an example of nonclassical acoustic nonlinearity in solids, Ultrasonics, **40**, 621-625 (2002).

[12] J. M. Richardson, Harmonic generation at an unbonded interface—I. Planar interface between semi-infinite elastic media, International Journal of Engineering Science, **17**, 73-85 (1979).

[13] P. Rajagopal and M. Lowe, Short range scattering of the fundamental shear horizontal guided wave mode normally incident at a through-thickness crack in an isotropic plate, The Journal of the Acoustical Society of America, **122**, 1527-1538 (2007).

[14] M. Castaings, E. Le Clezio, and B. Hosten, Modal decomposition method for modeling the interaction of Lamb waves with cracks, The Journal of the Acoustical Society of America, **112**, 2567-2582 (2002).

[15] P. J. Torvik, Reflection of Wave Trains in Semi‐Infinite Plates, The Journal of the Acoustical Society of America, **41**, 346-353 (1967).

[16] J. Achenbach and Y. Xu, Wave motion in an isotropic elastic layer generated by a time-harmonic point load of arbitrary direction, The Journal of the Acoustical Society of America, **106**, 83-90 (1999).